Catalytic performance of Rh/SiO_2 in glycerol reaction under hydrogen

Ippei Furikado, Tomohisa Miyazawa, Shuichi Koso, Akira Shimao,

Kimio Kunimori, Keiichi Tomishige*

Institute of Materials Science, University of Tsukuba

1-1-1, Tennodai, Tsukuba, Ibaraki 305-8573, Japan

Corresponding author: Keiichi Tomishige

Institute of Materials Science, University of Tsukuba

1-1-1 Tennodai, Tsukuba, Ibaraki, 305-8573, Japan

Tel and Fax: +81-29-853-5030

E-mail: tomi@tulip.sannet.ne.jp

Abstract

Glycerol is a main byproduct in a biodiesel production process, and the effective utilization of glycerol can contribute to the biodiesel promotion. One of the methods is catalytic conversion of glycerol to valuable chemicals, and this can also agree with the concept of green chemistry in terms of the utilization of renewable resources. Catalytic performance of supported metal catalysts (metal: Rh, Ru, Pt, Pd support: active carbon, SiO_2, Al_2O_3) was evaluated in the reaction of glycerol aqueous solution under H_2. It is found that Rh/SiO_2 exhibited higher activity and higher selectivity to hydrogenolysis products such as propanediols and propanols than Ru/C catalysts at low temperature (393 K). We also investigated the additive effect of ion-exchange resin (Amberlyst). Regarding the reaction route in the reaction of glycerol, it is suggested that the consecutive hydrogenolysis of propanediols to propanols on Rh/SiO_2 can proceed via 1,2-propanediol, while it can proceed on Ru/C via 1,3-propanediol.

1. Introduction

Catalytic conversion of renewable feedstock and chemicals becomes more and more important in terms of green chemistry. Such conversion to hydrogen can promote the utilization of renewable energy sources [1-5], and such conversion to petrochemicals can facilitate the replacement of petroleum by renewable resources [6,7,8]. It has been proposed that commodity chemicals derived from fossil resources at present will be producible in future biorefineries from renewable resources, such as plant-derived sugar and other compounds [9]. Glycerol is regarded as one of the building blocks in the biorefinery feedstock [9]. It has been also known as a main byproduct in the biodiesel production by transesterification of vegetable oils [10]. Attentions have been recently paid on the conversion of glycerol to petrochemicals such as propanediols[11] and acrolein[12,13]. Various catalysts have been attempted to the glycerol reaction to propanediols. The reaction formula is described below. The reaction corresponds to the substitution of the OH group with H_2, which is called here as hydrogenolysis.

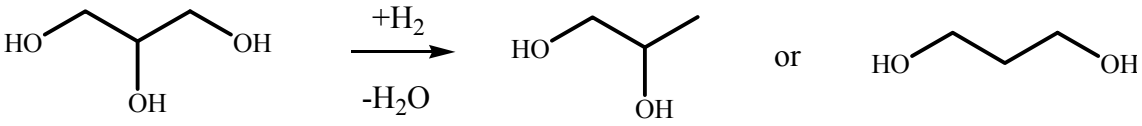

Using CuO/ZnO catalysts along with a sulfided Ru catalyst, the reaction of glycerol has been carried out at 15 MPa and 513-543 K [14,15]. Raney Cu [16,17], Cu/C [18] and Cu-Pt and Cu-Ru bimetallic catalysts [19] at 1.0-4.0 MPa and 493-513 K were also investigated. The catalysts containing Co, Cu, Mn, Mo, and inorganic polyacid were applied at the reaction conditions of 25 MPa and 523 K [20]. In the case of homogeneous catalysts containing W and group VIII transition metals, the reaction conditions were 32 MPa and 473 K [21]. Hydrogen pressures around 6-10 MPa and reaction temperatures of 453-513 K have been usually applied when supported metal catalysts were used [22-25]. In addition, it has been also reported recently that copper-chromite was effective for the hydrogenolysis of glycerol to 1,2-propanediol at 1.4 MPa and 473 K [26], which corresponded to the mild reaction condition in terms of hydrogen pressure. On the other hand, they also demonstrated that the copper-chromite catalyst exhibited lower activity below 453 K. It has been known that Ru/C showed rather high activity in the glycerol reaction in the presence of H_2 even at lower reaction temperature compared to the copper-chromite catalysts [27]. One of the weak points of Ru/C is that the degradation reaction as well as the hydrogenolysis can be also catalyzed in the glycerol reaction. The degradation reaction can be due to the cracking of the carbon-carbon bond. The reaction formula is shown below.

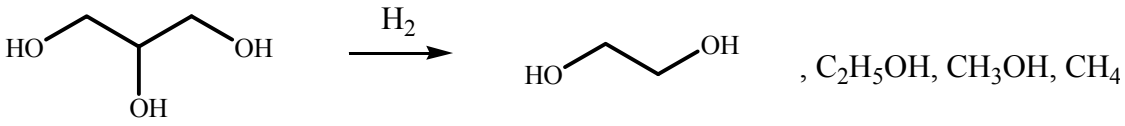

Since glycerol is regarded as a renewable source for the C_3 compounds, the aim of this study is the catalyst development for the hydrogenolysis reaction. Therefore, the degradation reaction is undesirable because it causes the decrease of the selectivity to the hydrogenolysis products. In this article, it is reported that Rh/SiO_2 gave higher yield of hydrogenolysis products and higher selectivity than Ru/C in the glycerol reaction in the presence of H_2. In addition, the additive effect of Amberlyst to Rh/SiO_2 was compared to the case of Ru/C. We also discuss the formation routes of

hydrogenolysis and degradation products based on the catalytic performance when the products in the glycerol reaction were used as reactants.

2. Experimental

Active carbon supported noble metal catalysts (Rh/C (BET surface area 557 m^2/g), Ru/C (485 m^2/g), Pt/C (478 m^2/g) and Pd/C (348 m^2/g)) were purchased from Wako Pure Chemical Industries; the loading amount of metal on these catalysts was 5 wt%. Noble-metal catalysts supported on Al_2O_3 and SiO_2 were prepared by impregnating the support materials with an aqueous solution of metal precursor such as $RhCl_3 \cdot 3H_2O$, $RuCl_3 \cdot 5H_2O$, $H_2PtCl_6 \cdot 6H_2O$, and $Pd(NO_3)_2$. These chemicals were supplied from Soekawa Chemical Co., Ltd. The loading amount of metal was 4 wt%. After the impregnation procedure and drying at 383 K for 12 h, they were calcined in air at 773 K for 3 h. The SiO_2 (G-6) (BET surface area 535 m^2/g) was supplied from Fuji Silysia Chemical Ltd. In addition, another SiO_2 (380) (380 m^2/g, Aerosil) was also used as a support material. The Al_2O_3 (JRC-ALO-1, 110 m^2/g) was supplied from Japan Reference Catalyst. The cation-exchange resin Amberlyst 15 (4.7 eq/kg-resin dried, particle size 0.4-1.2 mm, highest operating temperature 393 K; MP Biomedical) was used as a solid acid catalyst. All catalysts were used in powdery form with granule size of < 100 mesh.

The reaction of glycerol under H_2 atmosphere was carried out in a 70-ml stainless steel autoclave; a 20-ml aqueous solution of glycerol was used. The reaction was conducted under the following standard conditions: 393 K reaction temperature, 8.0 MPa initial hydrogen pressure, 10 h reaction time, 20 mass% glycerol aqueous solution, 150 mg supported metal catalyst with or without 300 mg Amberlyst. Catalysts were reduced in the reactor at 393 K for 1 h under 1.0 MPa H_2 pressure just before the activity test. Reaction conditions were changed for investigation of the reaction condition effect. Details of the reaction conditions are described for each result. In addition, we also carried out the reaction test of 1,3-propanediol(1,3-PD) and 1,2-propanediol(1,2-PD) in order to discuss the reaction routes of glycerol hydrogenolysis and degradation. The concentration

of these reactants of the aqueous solution was 2 mass%.

In all the experiments, the aqueous solution of the reactant, the catalyst powder and a spinner were put into the autoclave; then the reactor was purged with H_2 (99.99%; Takachiho Trading Co. Ltd.). After purging, the reactor was heated to the reaction temperature, and the H_2 pressure was increased. The temperature was monitored using a thermocouple that was inserted in the autoclave and connected to the thermo-controller. Although the hydrogen pressure decreased with reaction time, the decreased hydrogen pressure was 1/10 of the initial pressure at most. After the reaction, the gas-phase products were collected in a gasbag and the liquid phase products were separated from the catalyst powder through filtration. These products were analyzed using a gas chromatograph (Shimadzu GC-8A) equipped with FID. A Stabilwax capillary column (diameter 0.53 mmϕ, 60 m) was used for the separation. Products were also identified using GC-MS (QP5050, Shimadzu). As the products of the hydrogenolysis reaction, 1,2-PD, 1,3-PD, 1-propanol (1-PO) and 2-propanol (2-PO) were observed. As the products of the degradation reaction, ethylene glycol (EG), C_2H_5OH, CH_3OH and CH_4 were detected. Propanols were formed by the hydrogenolysis reaction of propanediols as below.

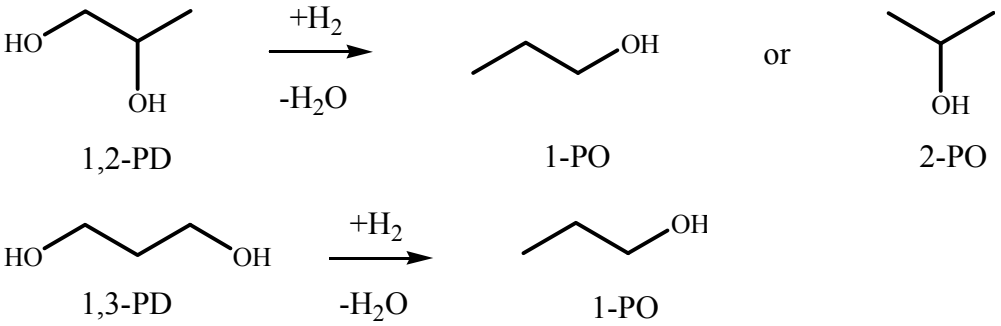

Conversion of the reactants in all reaction tests were calculated based on the following equation.

$$\text{Conversion of reactant (\%)} = \frac{\text{(Sum of C-based mol of all products)}}{\text{(Sum of C-based mol of reactant and all products)}} \times 100$$

The conversion can be also defined as (reactant before – reactant afterwards) / (reactant before)× 100. In the present case, it is necessary to determine the conversion and the selectivity even when the conversion level is very low. In addition, since all the products in the reaction tests were

identified, each values of the product amount were utilized, and the equation above was applied for the estimation of the conversion. It should be noted that the conversions calculated by this method and the method based on the definition agree well when the conversion was beyond around 5%. The mass balance was also confirmed in each result and the difference in mass balance was always in the range of the experimental error.

Selectivity of the products in all reaction tests were also calculated based on the following equation.

$$\text{Selectivity (\%)} = \frac{\text{(C-based mol of the product)}}{\text{(Sum of C-based mol of all products)}} \times 100$$

As a result of the reaction tests, ethylene glycol, ethanol, methanol and methane were detected as degradation products. The degradation of glycerol can give the C_2 and C_1 compounds in some cases. On the other hand, it can give only the C_1 compounds in other cases. Since the degradation can proceed in various ways, it is difficult to determine the formation route of each degradation product precisely. Therefore, we simply assume that each degradation product is formed from glycerol like $C_3 \rightarrow 3/2C_2$ and $C_3 \rightarrow 3C_1$ in the determination of the selectivity. The yield is calculated from Conversion (%) × Selectivity (%) / 100. The details are referred to our previous report [7]. The surface areas of the supported metal catalysts were measured using BET method (N_2 adsorption) with a Gemini (Micromeritics) apparatus. Temperature-programmed reduction (TPR) was carried out in a fix bed reactor equipped with a thermal conductivity detector using 5 % H_2 diluted with Ar (30 ml/min). The amount of catalyst was 0.05 g, and temperature was increased from room temperature to 1123 K at the heating rate of 10 K/min. Transmission electron microscope (TEM) images were taken for determination of the particle size using equipment (JEM 2010; JEOL) operated at 200 kV. After reduction with H_2, the samples were stored under vacuum until measurements were made. Supersonic waves dispersed the samples in 2-propanol, and dispersed samples were placed on Cu grids under air atmosphere. Average particle size was calculated by $\sum n_i d_i^3 / \sum n_i d_i^2$ (d_i: average particle size, n_i: number of particle with d_i)[28].

3. Results and discussion

The results of the glycerol reaction over various supported metal catalysts at 393 K are described in Figure 1. All the supported Pd and Pt catalysts exhibited very low activity in the glycerol reaction, and all the Al_2O_3 supported metal catalysts showed low activity. In the case of Ru catalysts, active carbon is much more suitable support than SiO_2 and Al_2O_3. This is also supported by the previous reports that Ru/C is an effective catalyst for the glycerol hydrogenolysis [7,17,23-25,27]. On the other hand, Ru/SiO_2 showed much lower activity than Ru/C. It should be noted that both Rh/SiO_2 of 380 and G-6 and Ru/C exhibited high activities for the glycerol reaction, in particular, Rh/SiO_2 (G-6) gave much higher yield of hydrogenolysis products than other catalysts, and the selectivity to hydrogenolysis products on Rh/SiO_2 (G-6) was higher than that on Ru/C. The product distribution is shown in detail later. Furthermore, the activity of Rh/Al_2O_3 was as low as that of other Al_2O_3 supported metal catalysts. In order to discuss the low activities of Al_2O_3 supported catalysts, the TPR profiles of SiO_2 and Al_2O_3 supported catalysts were compared as shown in Figure 2. The H_2 consumption peak of Rh/SiO_2 was clearly observed at 350 K, and, in contrast, that of Rh/Al_2O_3 was observed in the wide temperature range beyond 350 K. Here, we have to pay attention to the H_2 consumption behavior below the reduction pretreatment temperature and the reaction temperature of the glycerol reaction (393 K). The reduction degree below 393 K on the basis of $Rh^{3+} + 3/2H_2 \rightarrow Rh^0 + 3H^+$ is estimated to be 0.81 and 0.15 on Rh/SiO_2 and Rh/Al_2O_3, respectively. This suggests that the Rh species of Rh/SiO_2 can be reduced during the reduction pretreatment and the active metallic species is rich, however the Rh species of Rh/Al_2O_3 cannot be reduced sufficiently. From the results, the reducibility of Rh species on the support materials can influence the activity of the glycerol reaction strongly. On the other hand, the reduction of the Ru species on SiO_2 and Al_2O_3 proceeded above the reduction pretreatment and the reaction temperature (393 K). This result suggests that Ru species is not reduced and the active Ru metal species is not formed, and this can explain the low activity of Ru/SiO_2 and Ru/Al_2O_3. In the case of Pd/SiO_2 and

Pd/Al_2O_3, the H_2 consumption peak appeared in the range between room temperature and 400 K. The reduction degree on the basis of $Pd^{2+} + H_2 \rightarrow Pd^0 + 2H^+$ below 393 K was estimated to be 1.07 and 1.13 on Pd/SiO_2 and Pd/Al_2O_3, respectively. Two peaks observed on the TPR profiles of the Pd catalysts can be assigned to the reduction of Pd species with weak and strong interaction with the support surface. On the other hand, the peak intensity on Pt/SiO_2 and Pt/Al_2O_3 was very small. The Pt species on Pt/SiO_2 and Pt/Al_2O_3 are suggested to be reduced even at room temperature during the purge of the TPR cell with H_2 containing gas. These results suggest that major part of Pt and Pd can be reduced under the conditions of the glycerol reaction. On the other hand, all the SiO_2 and Al_2O_3 supported Pt and Pd catalysts showed very low activity in the glycerol reaction. This indicates that metallic Pt and Pd species is not so active. Regarding the active carbon supported catalysts, the metal species on all the catalysts can be reduced during the glycerol reactions because the peaks assigned to metal species were detected by X-ray diffraction method on the used samples as reported previously [7]. This also supports the low activity of Pt and Pd. In contrast, metallic Ru and Rh species are highly active, and these can be formed on Rh/SiO_2, Rh/C and Ru/C. In addition, the tendency in the activity over two Rh/SiO_2 and one Ru/C catalysts can be explained by the number of surface Rh atoms. From here, we focus on the catalytic performance of Rh/SiO_2 (G-6) and Ru/C.

Figure 3 shows the reaction temperature dependence of the glycerol reaction over Rh/SiO_2 (G-6) and Ru/C. It is characteristic that Rh/SiO_2 (G-6) exhibited lower selectivity to degradation products under higher glycerol conversion than Ru/C at 393 K. At higher reaction temperature, the selectivity to degradation products on Rh/SiO_2 (G-6) increased significantly. This result recommends that the reaction should be carried out at lower reaction temperature, where Rh/SiO_2 showed much higher activity and higher hydrogenolysis selectivity than Ru/C. As the details of the distribution of hydrogenolysis and degradation products are listed in Table 1, the main degradation products on Ru/C were EG and CH_4, and this represents the cracking of the C-C bond in the glycerol to ethylene glycol and methane. In contrast, in the case of Rh/SiO_2 (G-6), the selectivity to EG and ethanol were lower than that to CH_4. This indicates that the degradation reaction route on

Rh/SiO_2 is different from that on Ru/C, and this suggests that glycerol is cracked to three methane on Rh/SiO_2.

Figure 4 shows the effect of glycerol concentration over Rh/SiO_2 (G-6) and Ru/C. On both catalysts, the glycerol conversion decreased with increasing glycerol concentration. On the other hand, the difference between Rh/SiO_2 and Ru/C was larger at higher glycerol concentration, and it should be noted that Rh/SiO_2 gave higher glycerol conversion even under high glycerol concentration conditions. Although the details are not shown here, we confirmed that the reaction proceeded under steady-state conditions judging from the change of H_2 pressure during the test. Therefore it is possible to estimate the reaction rate from the results of the activity tests. In terms of the reaction rate of glycerol, the rate on Rh/SiO_2 was about twice as high as that on Ru/C under the condition of 40 mass% glycerol aqueous solution, although the difference was small at 2 mass% concentration. In addition, another important point is that Rh/SiO_2 maintained high selectivity to hydrogenolysis products even under high glycerol concentration.

Figure 5 shows the effect of H_2 pressure. At lower hydrogen pressure such as 2.0 MPa, Ru/C gave much higher glycerol conversion than Rh/SiO_2. In the case of the Ru/C, the effect of H_2 pressure was very small, and the yield of hydrogenolysis products increased gradually with increasing H_2 pressure. In contrast, in the case of Rh/SiO_2, the conversion and selectivity to the hydrogenolysis products increased remarkably with increasing H_2 pressure, and this means that the yield of hydrogenolysis products is enhanced by the increase of H_2 pressure. It is possible to estimate the reaction order of glycerol with respect to H_2 over Rh/SiO_2 (G-6), and the obtained order is estimated to be second. Further investigations on the promoting mechanism of hydrogen on the hydrogenolysis reaction over Rh/SiO_2 are necessary, however, the adsorbed hydrogen species on the Rh surface is suggested to promote the hydrogenolysis reaction.

Figure 6 shows TEM images of the used Rh/SiO_2 (G-6) and Ru/C catalysts after the reaction at 393 K for 10 h under the standard reaction conditions. The metal particles were observed in both cases, and the average particle size of Rh and Ru determined to be about 3.8 ± 0.2 and 2.5 ± 0.2 nm,

respectively. In the case of Ru/C, based on the relationship ($D = 1.32/d$) between particle size (d, nm) and the dispersion (D, %) [29, 30], the dispersion is calculated as 53 ± 4%. In the case of Rh/SiO_2 (G-6), based on the relationship, ($D = 1.10/d$)[29, 31], the dispersion is obtained as 29 ± 2%, which is lower than that of Ru/C. In addition, the average particle size of both catalysts after the reduction pretreatment were almost the same as those of used catalysts, although the details are not shown here. This means that the aggregation of metal particles during the reaction can be neglected, and this is related to the tendency that the decrease of H_2 pressure during the reaction was almost proportional to the reaction time. In addition, based on the dispersion obtained from the TEM results, the turnover frequency on Rh/SiO_2 (G-6) is estimated to be about five times as high as that on Ru/C under the standard reaction conditions.

Here, we investigated the effect of Amberlyst addition to Rh/SiO_2 (G-6) in the comparison with Ru/C. The results are listed in Table 1. In this experiment, the reaction temperature was chosen to be 393 K. One reason is based on the results of reaction temperature dependence (Figure 3), and another is due to the highest operating temperature of the ion-exchange resin. As reported previously, under the same reaction condition, the Amberlyst was stable for at least 60-hours [7]. From the comparison between Ru/C and Ru/C+Amberlyst, it is found that the glycerol conversion was increased by the addition of Amberlyst, and the total hydrogenolysis product yield mainly increased, in particular, 1,2-PD formation was drastically promoted. This behavior can be interpreted by the combination of the dehydration to acetol on Amberlyst and subsequent hydrogenation to 1,2-PD on Ru/C as reported previously [7]. On the other hand, in case of Rh/SiO_2 (G-6) and Rh/SiO_2 (G-6) + Amberlyst, the addition of Amberlyst enhanced glycerol conversion, and hydrogenolysis product yield, however, 1-PO formation was promoted most significantly. The propanediols are thought to be more valuable than propanols, the combination of Amberlyst with Ru/C can be more suitable than that with Rh/SiO_2.

In order to explain the product distribution, the reactions of 1,2- and 1,3-PDs under hydrogen were also tested (Table 2). On Ru/C and Ru/C+Amberlyst, the reaction rate of 1,3-PD was much

higher than that of glycerol and 1,2-PD, and this can be related to very low yield of 1,3-PD in the glycerol reaction. In contrast, the reaction rate of 1,2-PD was much lower than that of glycerol, and this is associated with high selectivity to 1,2-PD in the reaction of glycerol. In addition, the propanols are also formed by the sequential hydrogenolysis of propanediols. The hydrogenolysis of 1,2-PD can give 1-PO and 2-PO, and the hydrogenolysis of 1,3-PD can give 1-PO. The selectivity ratio of 1-PO to 2-PO is dependent on the catalysts. The selectivity to 1-PO was much higher than that to 2-PO in the reaction of glycerol over Ru/C and Ru/C+Amberlyst. The behavior indicates that 1-PO is mainly formed via 1,3-PD, whose amount was very low owing to its high reactivity over Ru/C and Ru/C+Amberlyst. High selectivity to C_2H_5OH on Ru/C and Ru/C+Amberlyst in the glycerol reaction also indicates that ethanol is formed from the degradation of propanediols. On the other hand, the reaction rate of 1,3-PD was comparable to that of glycerol over Rh/SiO_2 (G-6), and this can be related to much higher yield of 1,3-PD in the glycerol reaction than that on Ru/C, although the selectivity to 1,3-PD was not so high as that reported [20]. The selectivity ratio of 1-PO to 2-PO in the glycerol reaction on Rh/SiO_2 and Rh/SiO_2+Amberlyst seems to be similar to that in the reaction of 1,2-PD. This suggests that 1-PO is mainly formed via 1,2-PD, and this is different from that over Ru/C. By the Amberlyst addition to Rh/SiO_2, the formation of 1-PO was enhanced. This is because the Amberlyst catalyzes the dehydration of glycerol to acetol, as mentioned above, and Rh/SiO_2 catalyzes the hydrogenation of acetol to 1,2-PD, and furthermore Rh/SiO_2 catalyzes the hydrogenolysis of 1,2-PD to propanols with higher selectivity to 1-PO than 2-PO. Based on the results in Table 2, the model scheme of the glycerol reaction under H_2 over Ru/C and Rh/SiO_2 is described in Figure 6.

4. Conclusions

Among the various supported noble metal catalysts, it is found that Rh/SiO_2 (G-6) catalyst is effective in the reaction of glycerol under H_2. It is characteristic that Rh/SiO_2 exhibited higher activity and selectivity to hydrogenolysis products (1,2-PD+1,3-PD+1-PO+2-PD) in the reaction of

glycerol than Ru/C, which can be regarded as a conventional catalyst. In particular, under the higher H_2 pressure and higher concentration of glycerol, Rh/SiO_2 was more effective catalyst than Ru/C. By the addition of Amberlyst, glycerol conversion on the Rh/SiO_2 increased as well as on Ru/C. In addition, the reaction route of glycerol on Rh/SiO_2 can be different from that on Ru/C. The consecutive hydrogenolysis of propanediols to propanols in the glycerol reaction can proceed mainly via 1,3-propanediol on Ru/C, while the consecutive reactions can proceed mainly via 1,2-propanediol on Rh/SiO_2. The efficient catalytic conversion into valuable chemicals of glycerol, which is a main byproduct in the biodiesel production, can contribute to the promotion of biodiesel utilization in the economical view.

Acknowledgment

A part of this study is supported by Grant in Aid for Exploratory Research under the Japan Society for the Promotion of Science and Nippon Shokubai.

References

1 R. D. Cortright, R.R. Davda, J.A. Dumesic, *Nature*, 2002, **418**, 964.

2 G.W. Huber, J.W. Shabaker, J.A. Dumesic, *Science*, 2003, **300**, 2735.

3 G.A. Deluga, J.R. Salge, L.D. Schmidt, X.E. Verykios, *Science,* 2004, **303**, 993.

4 M. Asadullah, S. Ito, K. Kunimori, M. Yamada, K. Tomishige, *J. Catal.*, 2002, **208**, 255.

5 K. Tomishige, M. Asadullah, K. Kunimori, *Catal. Today*, 2004, **89**, 389.

6 G.W. Huber, J.N. Chheda, C.J. Barrett, J.A. Dumesic, *Science*, 2005, **308**, 1446.

7 T. Miyazawa, Y. Kusunoki, K. Kunimori, K. Tomishige, *J. Catal.*, 2006, **240**, 213.

8 T. Miyazawa, S. Koso, K. Kunimori, K. Tomishige, *Appl. Catal. A*, in press

9 S. Fernando, S. Adhikari, C. Chandrapal, N. Murali , *Energy Fuels*, 2006, **20**, 1727.

10 G. W. Huber, S. Iborra, A. Corma, *Chem. Rev.*, 2006, **106**, 4044.

11 T. Haas, B. Jaeger, R. Weber, S.F. Mitchell, *Appl. Catal. A*, 2005, **280**, 83.

12 M. Watanabe, T. Iida, Y. Aizawa, T.M. Alda, H. Inomata, *Bioresour. Technol.* 2007, **98**, 1285.

13 E. Tsukuda, S. Sato, R. Takahashi, T. Sodesawa, *Catal. Commun.*, in press

14 B. Casale, A.M. Gomez, US Patent 5,276,181 (1994).

15 B. Casale, A.M. Gomez, US Patent 5,214,219 (1993).

16 C. Montassier, D. Giraud, J. Barbier, J.P. Boitiaux, *Bull. Soc. Chim. Fr.*, 1989, **2**, 148.

17 C. Montassier, D. Giraud, J. Barbier, *Stud. Surf. Sci. Catal.*, 1988, **41**, 165.

18 C. Montassier, J.M. Dumas, P. Granger, J. Barbier, *Appl. Catal. A*, 1995, **121**, 231.

19 C. Montassier, J.C. Ménézo, J. Moukolo, J. Naja, L.C. Hoang, J. Barbier, *J. Mol. Catal.*, 1991, **70**, 65.

20 S. Ludwig, E. Manfred, US Patent 5, 616, 817 (1997).

21 C. Tessie, US Patent 4, 642, 394 (1987).

22 J. Chaminand, L. Djakovitch, P. Gallezot, P. Marion, C. Pinel, C. Rosier, *Green Chem.*, 2004, **6**, 359.

23 C. Montassier, J.C. Ménézo, L.C. Hoang, C. Renaud, J. Barbier, *J. Mol. Catal.*, 1991, **70**, 99.

24 D.G. Lahr, B.H. Shanks, *Ind. Eng. Chem. Res.*, 2003, **42**, 5467.

25 D.G. Lahr, B.H. Shanks, *J. Catal.*, 2005, **232**, 386.

26 M.A. Dasari, P.P. Kiatsimkul, W.R. Sutterlin, G.J. Suppes, *Appl. Catal. A*, 2005, **281**, 225.

27 Y. Kusunoki, T. Miyazawa, K. Kunimori, K. Tomishige, *Catal. Commun.*, 2006, **6**, 64.

28 Y. G. Chen, K. Tomishige, K. Yokoyama, K. Fujimoto, *J. Catal*., 1999, **184**, 479

29 J.R. Anderson, Structure of Metallic Catalyst, *Academic Press Inc.*, New York, 1975, p. 295.

30 A. Maroto-Valiente, M. Cerro-Alarcon, A. Guerrero-Ruiz, I. Rodriguez-Ramos, *Appl. Catal. A*, 2005, **283**, 23.

31 K. Kunimori, T. Uchijima, M. Yamada, H. Matsumoto, T. Hattori, Y. Murakami, *Appl. Catal.* 1982, **4**, 67.

Table 1. Result of the glycerol reaction over Rh/SiO_2(G-6) and Ru/C catalyst at 393 K[a]

Catalysts	Conversion (%)	Total yield of hydrogenolysis products (%)	Total yield of degradation products (%)	Selectivity of each product (%)[d]							
				1,2-PD	1,3-PD	1-PO	2-PO	EG	C_2H_5OH	CH_3OH	CH_4
Rh/SiO_2(G-6)+Amberlyst[b]	14.3	13.0	1.3	26.0	9.8	42.2	12.9	0.2	1.0	0.0	7.9
Rh/SiO_2(G-6)[c]	7.2	6.8	0.4	38.1	7.9	35.2	12.6	1.1	1.5	0.1	3.4
Ru/C+Amberlyst[b]	12.9	9.7	3.2	55.4	4.9	14.1	0.9	12.9	3.6	0.3	7.9
Ru/C[c]	3.5	2.0	1.5	26.4	4.9	26.7	0.3	22.0	5.8	2.3	11.6

[a] Reaction conditions: 20 mass% glycerol aqueous solution 20 ml, 393 K reaction temperature, 8.0 MPa initial H_2 pressure, 10 h reaction time.

[b] 150 mg metal catalyst + 300 mg Amberlyst

PD=propanediol, PO=propanol, EG=ethylene glycol.

[c] 150 mg

[d] C-based selectivity.

Table 2. Reaction results of various reactants over Rh/SiO_2 and Ru/C under H_2[a]

Catalysts	Reactant	Conversion (%)	Selectivity of each product (%)[d]							
			1,2-PD	1,3-PD	1-PO	2-PO	EG	C_2H_5OH	CH_3OH	CH_4
Rh/SiO_2(G-6)	Glycerol	29.3	22.6	5.4	41.3	17.0	0.0	1.8	0.0	12.0
+Amberlyst[b]	1,2-PD	17.5	-	0.0	56.5	21.6	0.0	2.1	0.0	19.7
	1,3-PD	22.6	0.0	-	68.2	0.0	0.0	6.8	0.0	24.9
Rh/SiO_2(G-6)[c]	Glycerol	19.6	34.6	5.2	39.1	13.7	0.0	2.9	0.0	4.6
	1,2-PD	9.8	-	0.0	66.5	20.9	0.0	1.0	0.0	11.6
	1,3-PD	19.2	0.0	-	81.3	0.0	0.0	9.3	0.0	9.4
Ru/C	Glycerol	38.8	28.8	0.8	28.9	2.4	7.4	18.7	1.9	11.2
+Amberlyst[b]	1,2-PD	6.3	-	0.0	28.2	30.0	0.0	27.8	0.0	13.9
	1,3-PD	77.7	0.0	-	32.8	0.0	0.0	44.8	0.0	22.4
Ru/C[c]	Glycerol	20.8	12.7	0.4	39.1	5.6	7.6	20.6	1.6	12.4
	1,2-PD	6.3	-	0.0	25.1	37.1	0.0	25.2	0.0	12.6
	1,3-PD	75.1	0.0	-	26.0	0.0	0.0	49.3	0.1	24.6

[a] Reaction conditions: 2 mass% aqueous solution of reactant 20 ml,
393 K reaction temperature, 8.0 MPa initial H_2 pressure, 10 h reaction time,
150 mg metal catalyst.

[b] 150 mg metal catalyst + 300 mg Amberlyst
PD=propanediol, PO=propanol, EG=ethylene glycol.

[c] 150 mg metal catalyst

[d] C-based selectivity.

Figure captions

Fig. 1. Results of glycerol reaction over supported noble metal catalysts at 393 K.
Reaction conditions: 20 mass% glycerol aqueous solution 20 ml,
8.0 MPa initial H_2 pressure, 10 h reaction time, 150 mg metal catalyst.
[a] Catalysts were reduced in-situ at 393 K and 1.0 MPa H_2.
[b] Catalysts were prereduced in the fixed bed reactor at 573 K and 0.1 MPa H_2,
and then the samples were transferred to the autoclave under air atmosphere.
[c] 1,2-propanediol +1,3-propanediol +1-propanol +2-propanol
[d] ethylene glycol +ethanol +methanol +methane

Fig. 2. Temperature-programmed reduction profiles of supported noble metal catalysts.
(a): SiO_2 (G-6) (b): Al_2O_3

Fig. 3. Reaction temperature dependence of the glycerol reaction over Rh/SiO_2 (G-6) (a) and Ru/C(b).
Reaction conditions: 20 mass% glycerol aqueous solution 20 ml,
8.0 MPa initial H_2 pressure, 10 h reaction time, 150 mg metal catalyst.
PD: propanediol, PO: propanol, others: ethylene glycol + ethanol + methanol + methane

Fig. 4. Effect of glycerol concentration in the glycerol reaction over Rh/SiO_2(a) and Ru/C(b).
Reaction conditions: 20 ml glycerol aqueous solution, 393 K reaction temperature,
8.0 MPa initial H_2 pressure, 10 h reaction time, 150 mg metal catalyst.
PD: propanediol, PO: propanol, others: ethylene glycol + ethanol + methanol + methane

Fig. 5. Effect of hydrogen pressure in the glycerol reaction over Rh/SiO_2(G-6) (a) and Ru/C(b).

Reaction conditions: 20 mass% glycerol aqueous solution 20 ml, 393 K reaction temperature, 10 h reaction time, 150 mg metal catalyst.

PD: propanediol, PO: propanol, others: ethylene glycol + ethanol + methanol + methane

Figure 6. TEM images of Rh/SiO_2 (G-6) (a) and Ru/C (b) catalysts after the glycerol reaction at 393 K for 10 h.

Figure 7. Model scheme of the glycerol reaction over Ru/C and Rh/SiO_2.

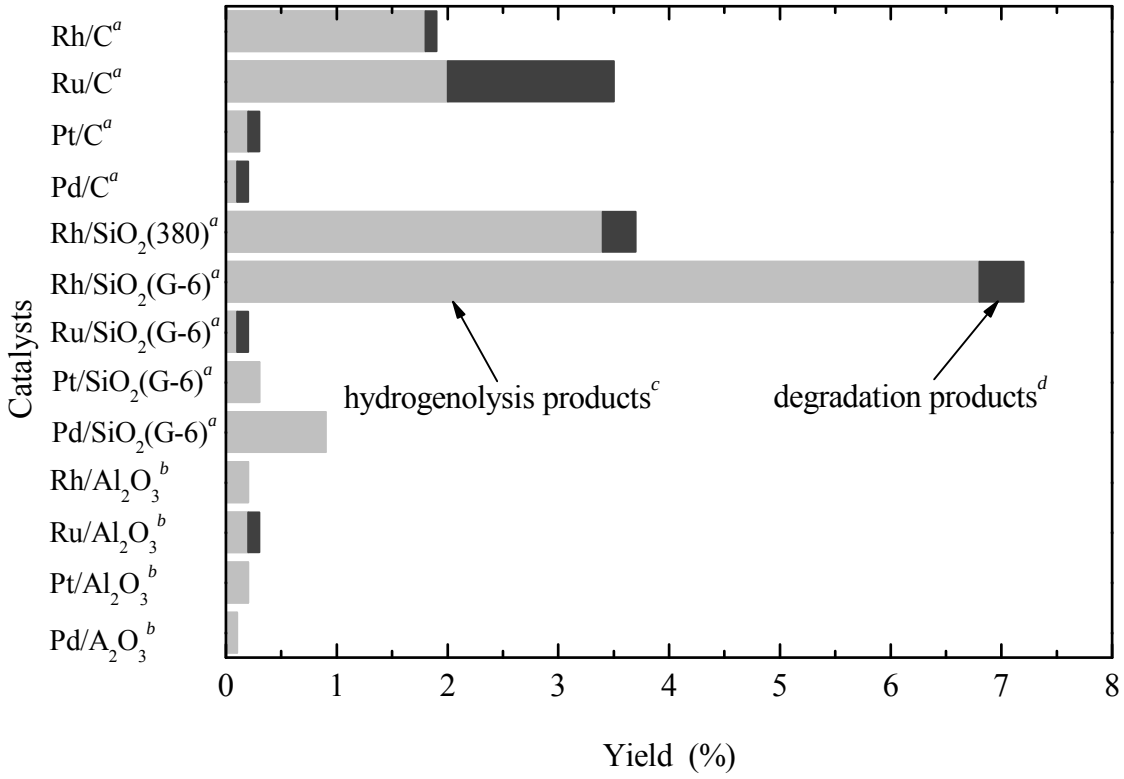

Figure 1. I. Furikado, et al.

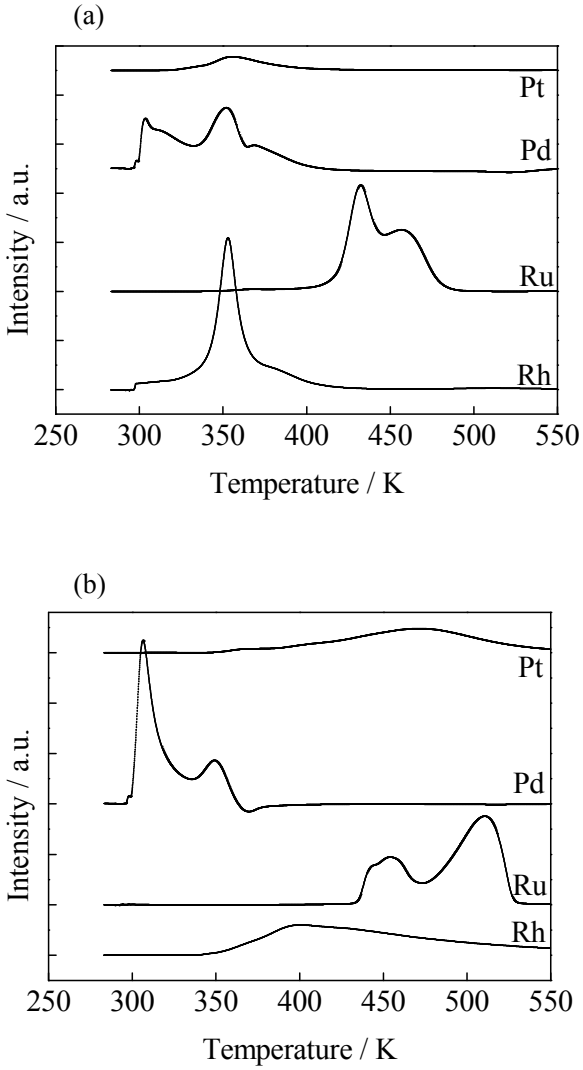

Figure 2. I. Furikado, et al.

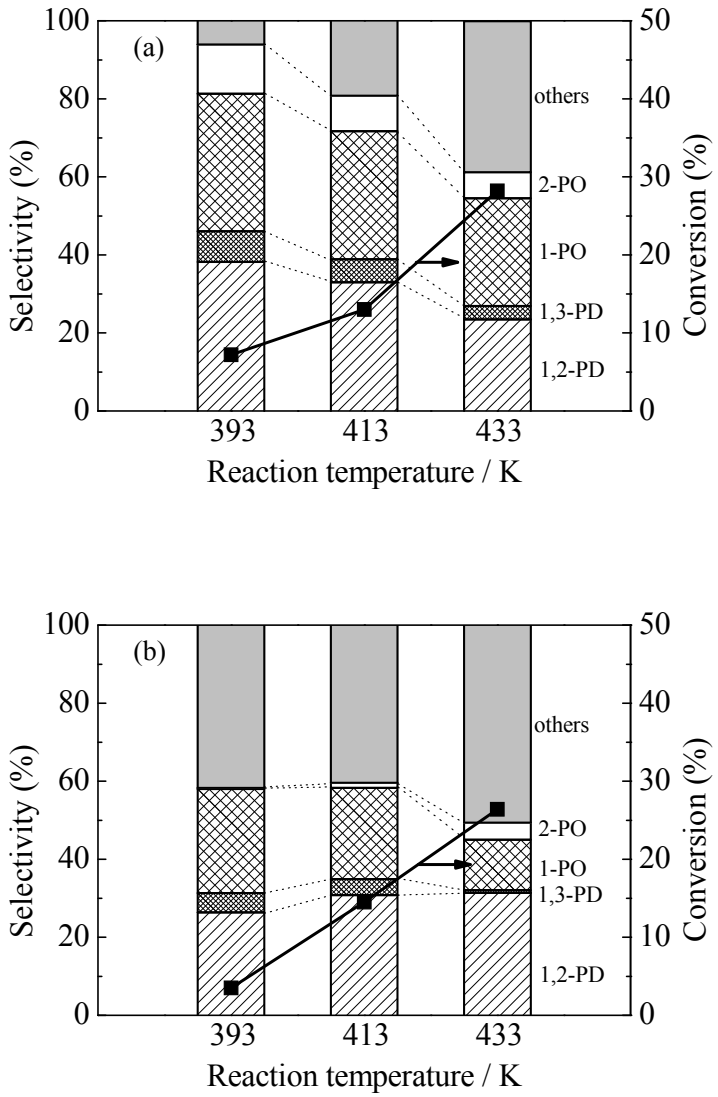

Figure 3. I. Furikado, et al.

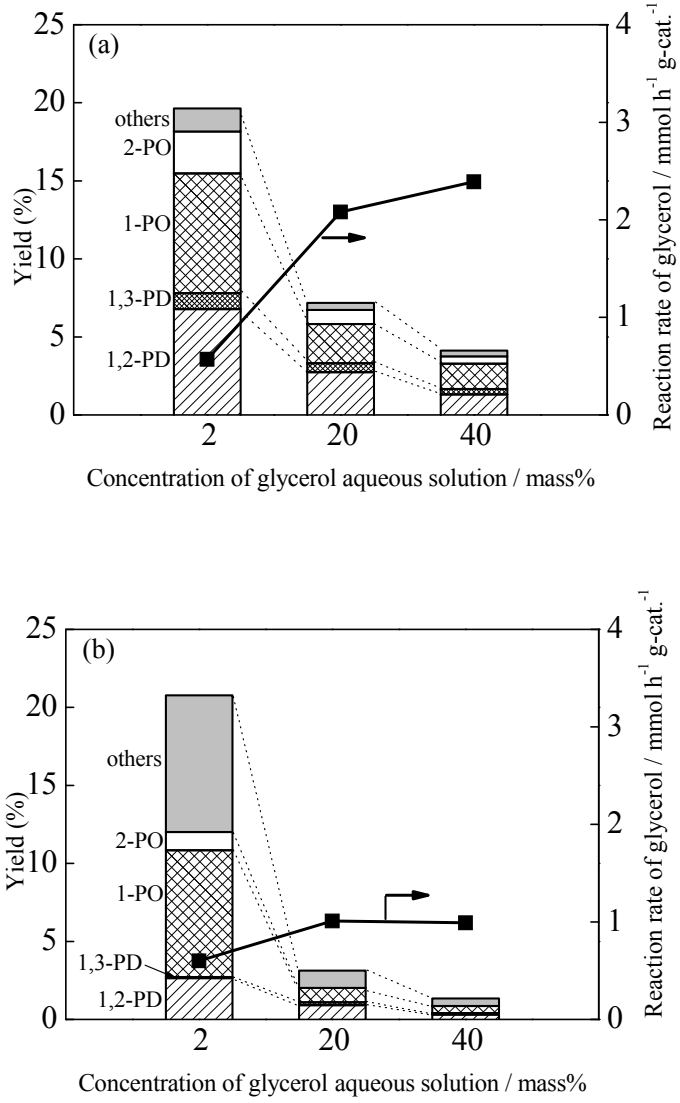

Figure 4. I. Furikado, et al.

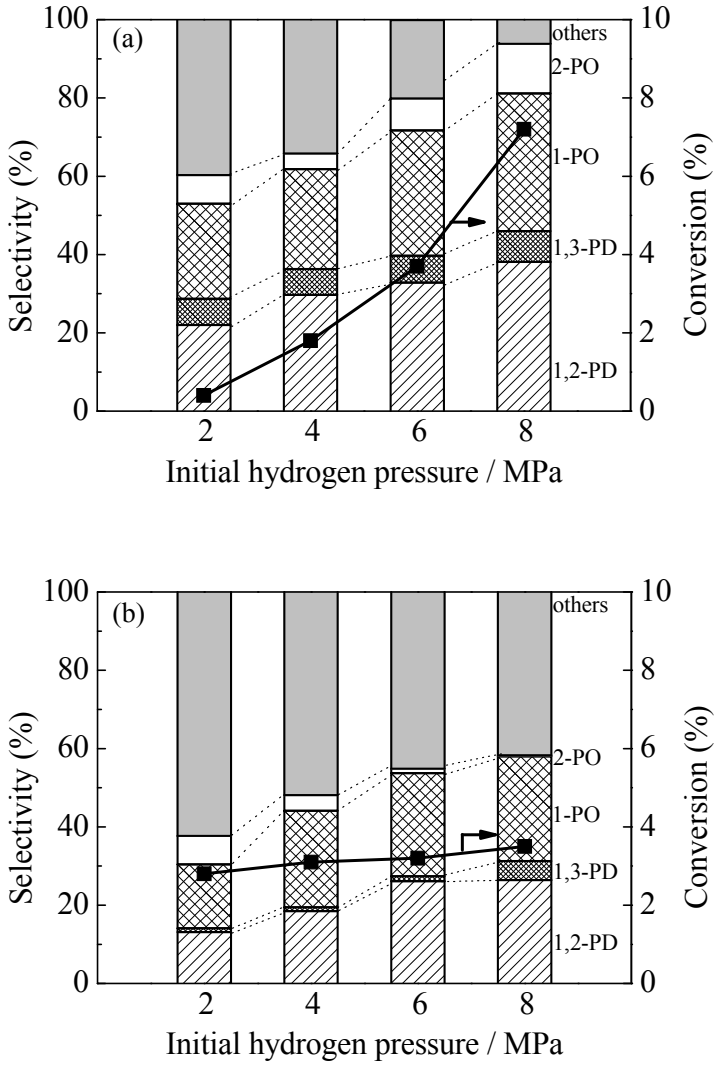

Figure 5. I. Furikado, et al.

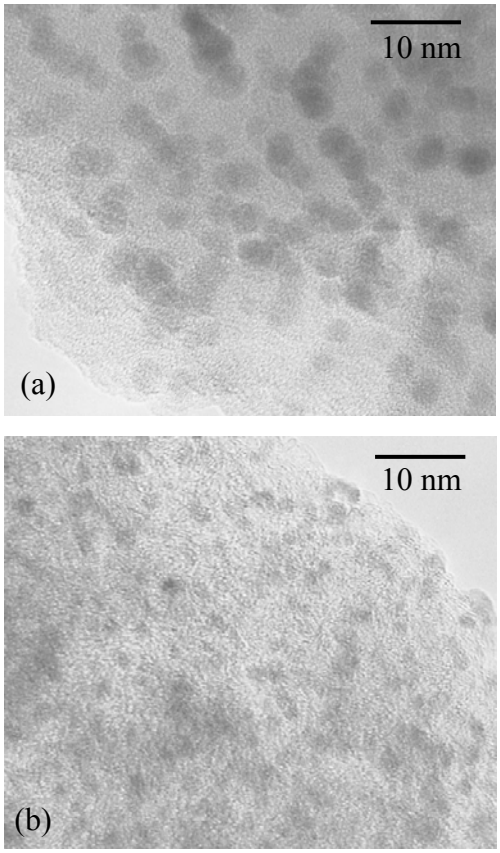

Figure 6. I. Furikado, et al.

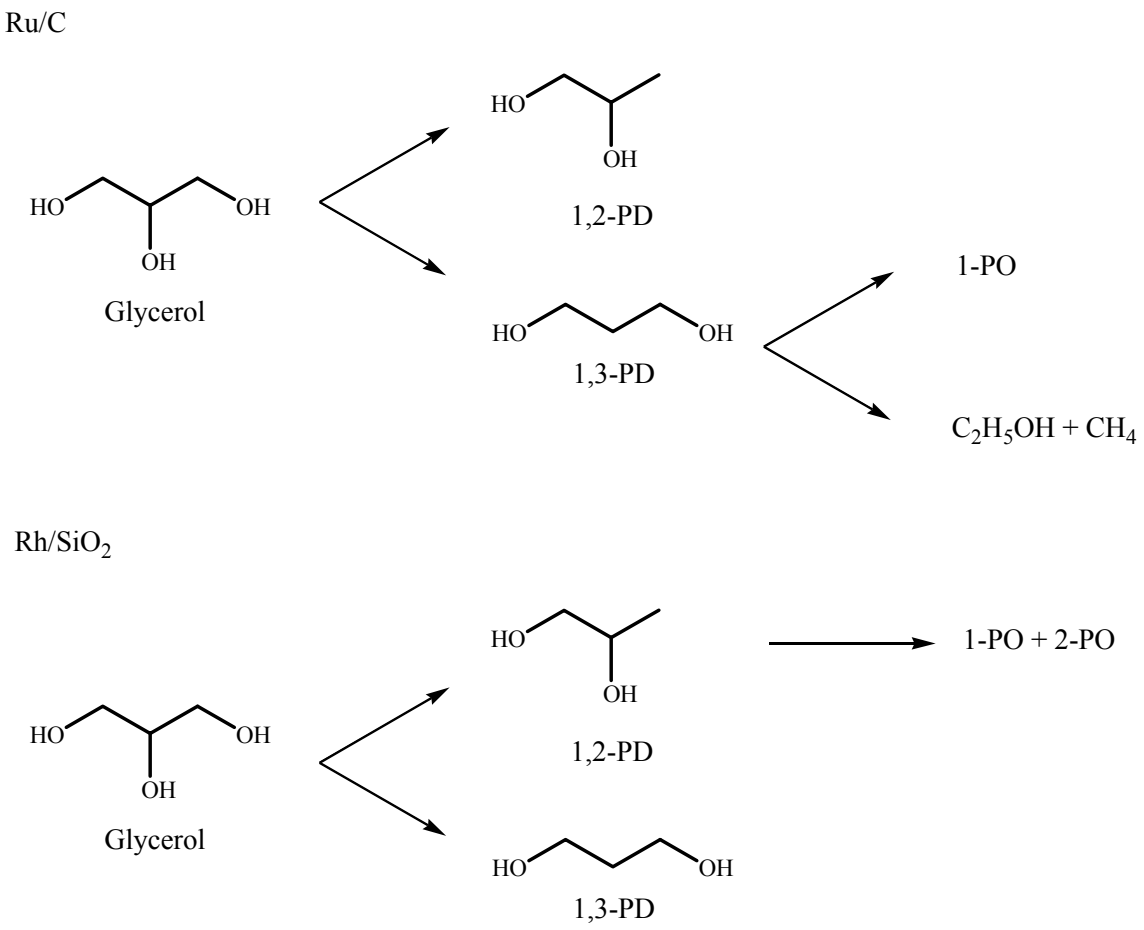

Figure 7. I. Furikado, et al.